Physics – Uspekhi **60** (8) 823 – 829 (2017)

CONFERENCES AND SYMPOSIA

PACS numbers: 04.25.dg, **04.30. – w**, 04.80.Nn, 95.55.Ym

First detections of gravitational waves emitted from binary black hole mergers

D H Reitze

DOI: https://doi.org/10.3367/UFNe.2016.11.038176

Contents

Abstract. The LIGO Scientific Collaboration and the Virgo Collaboration carried out the inaugural 'O1' observing run from September 12, 2015 through January 19, 2016 using the newly commissioned Advanced LIGO interferometers located in Hanford, WA and Livingston, LA. During the O1 run and the O2 run currently underway, three definitive detections of gravitational waves have occurred, each produced during the mergers of binary stellar mass black holes. A fourth candidate gravitational-wave event was identified, also likely produced from a binary black hole merger. The detected gravitational waveforms allow for the inference of the intrinsic astrophysical parameters of the merging binary systems, as well as the resulting black hole produced by the mergers. The first detect detections of gravitational waves confirm the existence of binary black hole systems and have profound implications for astrophysics using gravitational waves as a new and powerful probe of the universe.

Keywords: gravitational waves, general theory of relativity, laser interferometers, direct detection of gravitational waves, Advanced LIGO, Virgo

1. Introduction

Albert Einstein predicted the existence of gravitational waves in 1916 [1] as a natural consequence of his newly formulated General Theory of Relativity. Gravitational waves are time-dependent strains, $h = \Delta L/L$, that propagate at the speed of light and are produced by accelerating masses, or more precisely the second time derivative of the quadrupole mass moment of the source $\ddot{I}(t)$. The time-dependent strain from an accelerating massive object can be computed as $h(t) = 2G\ddot{I}(t)/rc^4$, where r is the distance from the source to the observer, and G, c are the Newtonian gravitational constant and vacuum speed of light, respectively. For the case of two spherical masses M separated by a distance $2R$ orbiting at a frequency f about each other, the strain amplitude is given by

$$h = \frac{32\pi^2 GMR^2 f^2}{rc^4}\,. \tag{1}$$

For approximately 50 years after Einstein predicted their existence, gravitational waves were treated as a curious but physically inconsequential afterthought of the theory [2], because their predicted amplitudes were incredibly tiny. Indeed, producing and detecting gravitational waves in a laboratory setting is hopeless with any technology available today or in the foreseeable future. Equation (1) predicts a strain of $\sim 10^{-35}$ for a dumbbell consisting of two 1000 kg masses separated by 1 m and rotating about its central axis 1000 times per second.

It was only in the 1960s that experimenters began searching for them from astrophysical sources. Unlike laboratory sources, it was conjectured at the time that gravitational waves from pulsars and supernovae might be possible to detect. Experiments using resonant bars to detect passing strains were carried out by Weber and others in the 1960s and 1970s [3] and, although in hindsight their sensitivities were incapable of detecting astrophysical sources by many orders of magnitude, these detectors and the physicists who built them were trailblazing, calling attention to the possibility of being able to detect gravitational waves with an earth-based detection apparatus.

The nascent field of gravitational-wave detection received another boost in 1962 with the publication of a paper by

D H Reitze. LIGO Laboratory, California Institute of Technology, MS 100-36, Pasadena, CA 91125, USA
E-mail: reitze@ligo.caltech.edu

Received 7 July 2017
Uspekhi Fizicheskikh Nauk **187** (8) 884 – 891 (2017)
DOI: https://doi.org/10.3367/UFNr.2016.11.038176
Edited by K A Postnov

Gertsenshtein and Pustovoit [4], which postulated that an interferometer could, in principle, be a better detector for gravitational-wave strains.* Weiss explored interferometric gravitational-wave detection in a comprehensive fashion in 1972 [5], producing the first serious design for an interferometric gravitational-wave antenna, as well as a careful theoretical investigation of the fundamental noises that ultimately limit the sensitivity of an interferometer.

2. LIGO interferometers

The Laser Interferometer Gravitational-wave Observatory (LIGO) grew out of the initial efforts of Weiss, as well the work of Drever [6] and others [7].

LIGO comprises two essentially identical observatories located in Hanford, WA USA (designated H1) (Fig. 1a) and Livingston, LA USA (L1). Each observatory houses an interferometer with arm lengths of 4 km and with much of the interferometer infrastructure and the arms located in a $10^{-8}-10^{-9}$ Torr high vacuum system.

The LIGO Observatories were built in 1995–1998, and the initial generation of LIGO interferometers was completed in 2002. From 2002–2010, a series of scientific runs was carried out to search for gravitational waves, with the detectors reaching what was at the time an unprecedented rms strain sensitivity $h_{\rm rms} < 10^{-21}$ measured in a narrow frequency band centered on 100 Hz. This strain corresponds to an rms displacement sensitivity $\Delta L_{\rm rms} \sim 10^{-18}$ m. While ultimately these searches did not detect gravitational waves, the most stringent upper limits were established for the primordial gravitational-wave background from the Big Bang and on gravitational-wave emissions from galactic pulsars. Following the initial science runs, the LIGO detectors underwent a redesign and rebuild in which each interferometer was completely reconstructed. The result was Advanced LIGO, a second-generation detector designed to be 10 times more sensitive than the initial LIGO interferometers. After a five-year period of construction and commissioning, the two LIGO interferometers began scientific operations in September 2015.

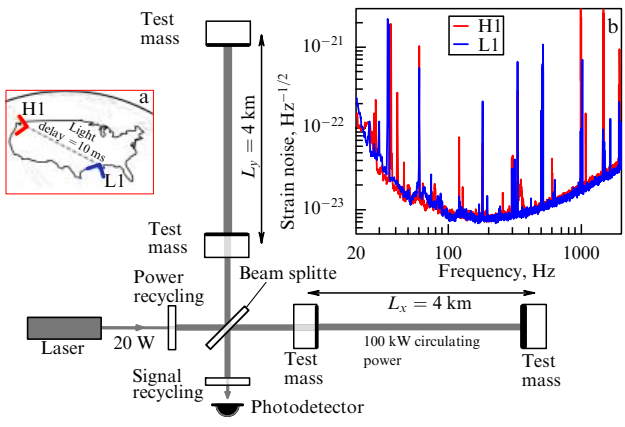

Figure 1. Advanced LIGO interferometers. Figure 1a displays the physical location of the two interferometers in Hanford, WA and Livingston, LA USA. A simplified version of the overall interferometer layout is displayed in the center, showing the laser, the central Michelson interferometer consisting of the beamsplitter and the input test masses, the 4-km-long Fabry–Pérot arm cavities, the power- and signal-recycling mirrors, and the detection photodiode. For the first 'O1' observing run, 20W of laser power was injected into the interferometer, resulting in 100 KW in the arm cavities. The typical measured strain noise spectra for the Hanford (red) and Livingston (blue) interferometers are shown in the upper right. (Taken from Ref. [98]).

A complete description of the Advanced LIGO interferometers can be found in reference [9]. Here, we describe simply and in broad terms the operational principles of the interferometers and their designs. A gravitational wave propagating in the z-direction produces a time-dependent strain in the x- and y-directions for the h_+ polarization (or 45° to the x- and y-directions for the $h_\times$ polarization). An interferometer will experience a time-dependent differential displacement as a gravitational wave passes, producing a signal on the detection photodiode located at the output port of the interferometer (see Fig. 1). The magnitude of the signal depends not only on the intrinsic gravitational-wave strain amplitude at the detector, but also on the direction of propagation relative to the xy-plane defined by the interferometer arms, with signals decreasing in strength with respect to the optimal z-propagation direction or with strains maximally aligned with the interferometer arms.

The optical layout of the LIGO interferometers (see Fig. 1) is based upon the simple Michelson interferometer, comprising a laser, a beamsplitter, and two end mirrors ('test masses'). To achieve the requisite sensitivity, however, several modifications have been implemented which enhance the accumulated signal from a passing gravitational wave. The 4-km-long arms are fitted with Fabry–Pérot cavities to increase the storage time of laser light in the interferometer. The interaction time between the laser light and the gravitational wave and hence the relative time delay that the light experiences between the x- and y-arms of the interferometers is increased by the effective number of round trips the light experiences in the cavity. Alternatively, the presence of Fabry–Pérot cavities in the arms can be thought of as amplifying the phase shift of light for a given displacement, $\Delta\phi_{\rm FP} = (2F/\pi)\,\Delta\phi_{\rm Mich}$, where F is the finesse of the cavity and $\Delta\phi_{\rm Mich}$ is the simple Michelson phase shift.[1] Under quiescent conditions, the differential displacement $\Delta L = L_y - L_x$ is set to constructively interfere light arriving at the beamsplitter back toward the laser. The addition of an interferometrically positioned 'power recycling' mirror allows another resonant cavity to be formed, comprising the power recycling mirror and the 'complex' mirror formed by the Michelson interferometer with Fabry–Pérot arm cavities. This results in increased light power on the beamsplitter by the power-recycling cavity gain, which in turn increases the signal-to-noise ratio relative to shot noise.

A final cavity, the signal-recycling cavity, is formed by placing a mirror between the beamsplitter and the sensing photodiode. The position of signal recycling mirror can be set either to recirculate the gravitational-wave sidebands generated by the passing gravitational waves back into the interferometer to enhance the signal (as the name suggests) or to extract the signal from the interferometer ('resonant sideband extraction'). Collectively, these enhancements pro-

* Prospects of GW detection by laser interferometers were soon recognized in one of the first reviews devoted to the possible experimental discovery of gravitational waves [see Braginskii V B "Gravitational radiation and the prospect of its experimental discovery" *Sov. Phys. Usp.* **8** 513 (1966)]. (*Editor's note.*)

[1] Technically, this is only true in the limit where the gravitational wave period is long compared with FL/c, the effective light travel time in the Fabry–Pérot cavities.

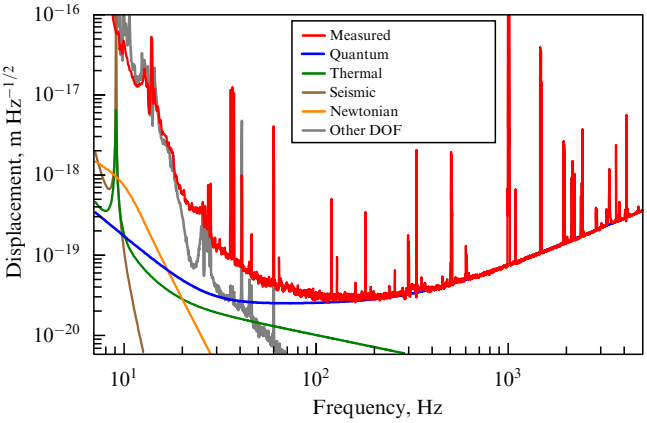

Figure 2. Typical noise spectrum for the H1 interferometer for LIGO's first 'O1' observing run. The red curve is the measured sensitivity, calibrated as displacement amplitude spectral density. Predicted (modeled) levels of noise (blue, green, brown, orange) and measured noises (gray) are compared to the measured sensitivity. There is good agreement between the detector performance and the predicted/measured noises except in the 20–100 Hz frequency band, where an excess of unknown noise is present. (Taken from Ref. [10]).

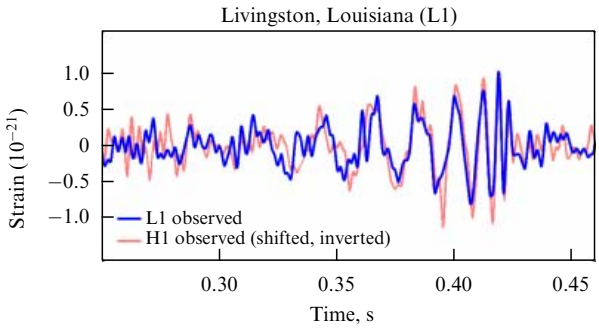

Figure 3. Comparison of the measured strain for the Livingston L1 detector (blue) and Hanford H1 detector (red). The H1 strain curve is inverted to account for the relative orientation with the L1 detector and shifted in time by 6.9 ms to account for the arrival time difference. (Taken from Ref. [8].)

vide orders of magnitude more sensitivity when compared with a simple Michelson interferometer.

The interferometer must be made as immune as possible to any physical perturbations that produce false signals with an amplitude comparable to the desired gravitational wave signal sensitivity. These perturbations fall into three categories: i) fundamental sensing noises that alter the arrival time of the light relative to the time determined purely by the passing of a gravitational wave, ii) fundamental displacement forces that physically move the mirrors by a length ΔL, and iii) technical noises that arise from sensors and actuators embedded in servo control loops, electronics noise, laser frequency/amplitude/pointing fluctuations, and a large number of other contributors. The fundamental noises are dictated by the underlying physics and the choice of design parameters — the laser power, the mass of the mirrors, the mirror and optical coating materials, the local ground motion, and ultimately 'Newtonian' (dynamic gravity gradient) noise and phase noise due to light scattering from the residual gas in the evacuated beam tubes. Figure 2 displays a representative displacement noise spectrum for the Hanford 'H1' interferometer during the O1 run, including contributions from the primary noise sources. The underlying individual noises are assumed to be uncorrelated with one another, and are added in quadrature to produce the predicted noise performance. Over most of the frequency band, the measured noise agrees well with the modeled and independently measured noises, with the exception of the 20–100 Hz region, in which unknown excess noise is present. Understanding and eliminating the sources of this noise is an area of active investigation.

3. First direct detections of gravitational waves from binary black hole mergers

The first Advanced LIGO observing O1 run was carried out between September 12, 2015 and January 19, 2016, after a six-month (13-month) commissioning period for the H1 (L1) interferometer. Remarkably, a very strong coincident trigger was detected during an engineering phase on September 14, 2015 at 09:50:45 UTC by a low latency data analysis pipeline designed to search for transient gravitational-wave signals using a model-independent algorithm [11]. The event candidate, named GW150914, possessed a sufficiently high signal-to-noise ratio (SNR) that it could be observed in the raw minimally filtered data stream for both the H1 and L1 detectors. The H1 and L1 signals had very similar morphologies (Fig. 3), and were consistent with a waveform produced by two compact massive objects which inspiral and merge to form a more massive object. The signal at L1 was recorded 6.9 ms in advance of H1, within the inter-observatory propagation delay time. A careful examination of the data quality and detector performance around the time of the candidate revealed no anomalies [12].

The LIGO Scientific Collaboration (LSC) and Virgo Collaboration (VC) performed a comprehensive analysis of GW150914 as a gravitational-wave candidate. Here, I highlight some of the key investigations and findings, including an assessment of the statistical confidence of the candidate, determination of the physical characteristics of the signal, and comparisons of the detected waveforms with what General Relativity would predict for gravitational-wave emission. A comprehensive treatment is beyond the scope of this article; however, a broad suite of results can be found in Refs [8, 12–16].

3.1 GW150914: search/analysis methods and results

Multiple search methods have been developed and refined for identifying gravitational-wave transients and quantifying their statistical significance. Search algorithms fall into two categories — template-based searches for gravitational waveforms (relying on underlying physical models for GW generation from compact binary inspiral and merger) and model-independent searches (that make minimal assumptions about the waveform morphology). Template-based searches use matched filter techniques that are inherently more sensitive (matched filtering is the optimal method for finding signals buried in noise), relying on analytical or numerical waveforms produced from compact binary inspirals/mergers.** Model-independent searches search for excess power contained in specific time/frequency bins, and can

** Physical principles and details of calculations of GW waveforms from coalescing compact binaries were recently reviewed in *Physics-Uspekhi* by M.A. Sheel and K.S. Thorne [see "Geometrodynamics: the nonlinear dynamics of curved spacetime", *Phys. Usp.* **57** 342 (2014)]. (*Editor's note*.)

identify a broader class of GW signals at the expense of reduced search sensitivity. The LSC and VC employed both types of searches during the O1 run.

Three independent pipelines — two template-based searches [17, 18] and one using a wavelet-based model-independent algorithm [11] — were used to validate GW150914 and determine its statistical significance. Determining the significance of one or more candidate events requires a quantitative estimation of the background rate of triggers. Obstacles to determining the background are two-fold. First, interferometer noise is non-Gaussian, with nonstationary temporal transients (or 'glitches') occurring in the data due to a variety of instrumental and environmental causes. Second, the LIGO detectors cannot be shielded from gravitational waves; thus, it is impossible to produce a signal-free background. The background is determined empirically, generated by replicating the data a large number of times through time shifting of the Livingston data $h(t+T)$ stream relative to Hanford's $h(t)$ state in excess of the inter-site coincidence time, and repeating the searches on this 'nonastrophysical' data set. A gravitational wave requires a temporal coincidence between the two LIGO observatories less than or equal to the inter-site light travel time. Additionally, template-based searches use 'χ^2-tests' to compare the measured waveform with the known time-frequency evolution of the inspiral signal, allowing a further reduction in the background [19].

Figure 4 presents the results of a 'pyCBC' template-based search. The analysis used 16 days of two-detector coincidence data, with $\sim 10^7$ time shifts applied to produce a background duration corresponding to roughly 6.08×10^5 years. The background is computed in two ways — by leaving GW150914 in the time-shifted background (black line) and by removing it (purple line). The former approach is more conservative, producing a detection statistic (related to the event signal to noise ratio) of 23.6. Because GW150914 is (by far) the loudest event, only an upper bound was placed on the false alarm rate (1 in 6.08×10^5 years). A 'gstLAL' template-based search produces similar results. The model-independent analysis leads to a slightly less significant event of 1 in 2.2×10^4 years. Subsequent reanalysis of GW150914 using a refined detector calibration and a longer background data set led to a revised detection statistic of 22.7 and false alarm rate of 1 in 1.67×10^6 years [20].

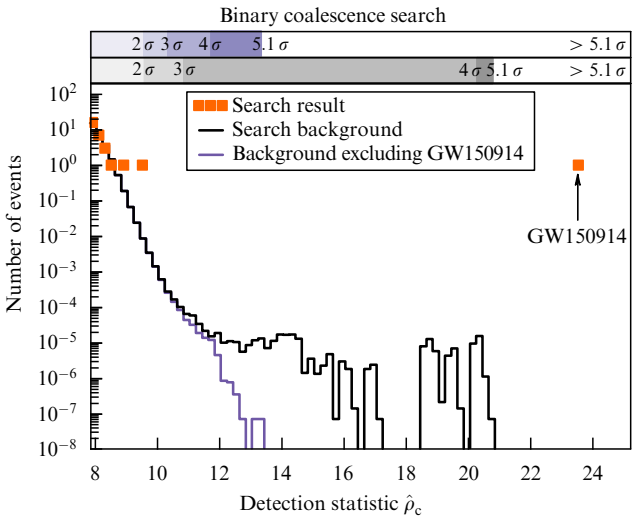

Figure 4. Results from the pyCBC binary coalescence template-based search, plotting the number of event candidates (orange squares) and backgrounds as a function of the detection statistic. The two backgrounds are computed with GW150914 included in (black line) or removed from (purple line) the time-shifted data.

Table 1. Estimated physical parameters of GW150914.[2] All values are given in the source frame of the merger. Black hole spins are given in the terms of the dimensionless spin parameter $a = c|\mathbf{S}|/(Gm^2)$.

Primary black hole mass, $m_1/M_\odot$	$36.2^{+5.2}_{-3.8}$
Secondary black hole mass, $m_2/M_\odot$	$29.1^{+3.7}_{-4.4}$
Final black hole mass, $m_f/M_\odot$	$62.3^{+3.7}_{-3.1}$
Final black hole spin, a_f	$0.67^{+0.05}_{-0.06}$
Radiated gravitational-wave energy, $M_\odot c^2$	$3.0^{+0.5}_{-0.4}$
Peak luminosity FV, erg s^{-1}	$3.6^{+0.5}_{-0.4} \times 10^{56}$
Luminosity distance, D_L, Mpc	420^{+150}_{-180}
Redshift z	$0.09^{+0.03}_{-0.04}$

3.2 Determination of the astrophysical parameters of GW150914

Astrophysical information is encoded in the morphologies of the GW150914 waveform, as well as in the relative arrival time delay at the two interferometers. To infer these parameters from the waveform data, a Bayesian analysis is performed. Information about the source properties is determined by the probability distribution function (PDF) $p(\boldsymbol{\theta}|\boldsymbol{d})$ of obtaining source parameters $\boldsymbol{\theta}$ given the measured waveform data stream $\boldsymbol{d}$. The PDF is computed using coherent Bayesian inference techniques incorporating model selection algorithms for different families of binary black hole merger waveforms. Given the complete lack of astrophysical constraints on BH mergers, the priors on the source parameters are taken to be uniform. More details can be found in references [14, 21].

An isolated coalescing binary black hole system is described by its intrinsic source parameters — the two component masses m_1 and m_2 with spins $\mathbf{S}_1$ and $\mathbf{S}_2$ — as well as extrinsic parameters such as luminosity distance D_L, sky location angles (α, δ), the orbital inclination i relative to the interferometer planes, polarization, merger time t_c, and the phase. The key source parameters for GW150914 that can be extracted from the data are given in Table 1. The error bars represent the 90% credible intervals for the parameters, and include both statistical errors and systematic errors arising from averaging the results of different waveform models.

3.3 GW150914 consistent with general relativity

The detected waveforms carry important information about the nature of general relativity and provide an opportunity to test its validity in the dynamical strong-field regime where v/c becomes nonnegligible. At the moment before coalescence, the two black holes possessed orbital velocities exceeding half of the speed of light. Several investigations were performed to test whether GW150914 was consistent with the predictions of general relativity and search for any deviations [16].

Figure 5 compares the reconstructed gravitational-wave strain data for Hanford and Livingston (after subtracting residuals consistent with detector noise) with the best matched numerical relativity simulations of the detected

[2] These values are based on reanalysis of the data as presented in Ref. [20], and differ slightly from those reported in Ref. [8].

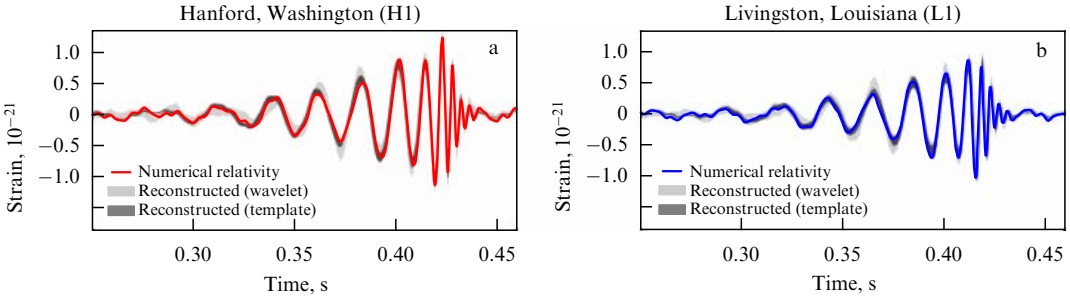

Figure 5. Comparison of the Hanford (left) and Livingston (right) reconstructed gravitational waveforms with numerical relativity. The light gray (dark gray) curve presents the reconstruction using wavelets (compact binary merger templates); the colored curves are numerical relativity simulations using parameters for GW150914.

waveforms. Two reconstructions are compared to each NR result, corresponding to the template-based and model-independent (wavelet-based) searches. The reconstructions have almost 95% overlap with the NR waveforms, suggesting that if deviations exist with respect to general relativity, they are small and within the noise of the measurement.

An additional general relativity consistency test can be performed using a generalized parameterization of the post-Newtonian (PN) approximation for the gravitational waveform and comparing it with the measured phase evolution of the signal. Any deviations from general relativity would be manifested as nonzero values for the parameters. Within 90% confidence limits, no deviations from the PN expansion up to order 3.5 PN (the maximum order used in the waveform models) are found, placing upper bounds on the deviations significantly better than those obtained from the double pulsar system J0737-3039 [22], with the exception of the 0PN order.[3]

Finally, it is possible to put an upper limit of the rest mass of graviton m_g. The graviton's mass is related to its Compton wavelength as $\lambda_g = h/(m_g c)$, where h is Planck's constant. The frequency-dependent gravitational-wave phase can be modified to include a massive graviton term [23]:

$$\Psi_{\rm MG}(f) = \Psi_{\rm GR}(f) - \frac{\pi^2 DM}{\lambda_g^2(1+z)}\,(\pi M f)^{-1}\,, \qquad (2)$$

where $\Psi_{\rm GR}$ is the standard post-Newtonian phase term, D is the source distance computed in flat space-time assuming standard ΛCDM cosmology, and $M = m_1 + m_2$. A finite Compton wavelength would be manifested as dispersive propagation of the gravitational waves, producing a phase deviation with respect to standard General Relativity in the measured waveforms. Using methods akin to those described in Section 3.2, standard binary black hole merger waveform models are modified to include the massive graviton term and tested using Bayesian inference to produce a cumulative probability distribution for λ_g. A 90% confidence level upper limit of $\lambda_g > 10^{13}$ km is found, corresponding to $m_g \leqslant 1.2 \times 10^{-22}$ eV/c^2. While this upper limit is less than those obtained from weak gravitational lensing and other methods, it is nonetheless the most stringent upper limit obtained in the highly relativistic strong field gravity regime.

[3] The 0PN upper bound in J0737-3039 benefits from a 10-year observation period by radio telescopes, as opposed to a < 1 s observation time with GW150914.

3.4 GW151226, GW170104, and LVT101226: two (and probably three) more binary black hole mergers

A second confirmed gravitational wave event was detected on December 26, 2015 at 03:38:53 UTC during the O1 run [24]. GW151226 was also first found by low latency search pipelines and subsequently confirmed as a binary black hole merger with a network SNR of 13.0 and a false alarm rate of less than 1 in 1.67×10^6 years. Because the black holes possessed lighter masses (approximately14.2 and 7.5 solar masses, respectively), they merge at a higher frequency and spend more time in the LIGO interferometers' frequency band. Approximately 55 cycles of the inspiral and merger phase of GW151226 are captured over a 1.5-second period (Fig. 6), corresponding to ~ 27 orbital periods. (For comparison, GW1501914 had only 10 cycles.)

LIGO's O2 run, which began on November 30, 2016, yielded a third gravitational wave detection emanating from a binary merger of two black holes [25]. GW170104 was detected on January 4, 2017 at 10:11:58.6 UTC with initial component masses between the two earlier detections. Located at a distance of 880 Mpc, GW170104 is to date the most distant black hole merger ever confirmed. Unlike the two previous detections, GW170104 is the first merger revealing evidence that the merging black hole spins are not

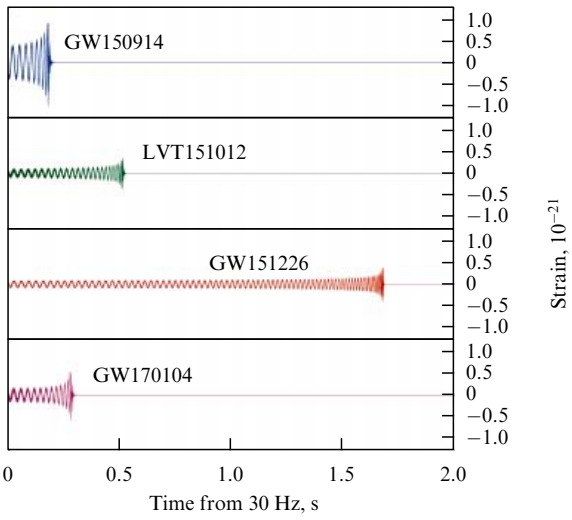

Figure 6. Waveform reconstructions of the three confirmed gravitational-wave detections and the less statistically significant event candidate displayed as a function of time, referenced from the time the signals cross into the LIGO interferometers' frequency band at 30 Hz.

Table 2. Estimated physical parameters of GW151226, GW170104, and LVT151012. All values are given in the source frame of the merger.

	GW151226	GW170104	LVT151012
Primary black hole mass, $m_1/M_\odot$	$14.2^{+8.3}_{-3.7}$	$31.2^{+8.4}_{-6.0}$	23^{+18}_{-6}
Secondary black hole mass, $m_2/M_\odot$	$7.5^{+2.3}_{-2.3}$	$19.3^{+5.3}_{-5.9}$	13^{+4}_{-5}
Final black hole mass, $m_f/M_\odot$	$20.8^{+6.1}_{-1.7}$	$48.7^{+5.4}_{-4.6}$	35^{+14}_{-4}
Final black hole spin a_f	$0.74^{+0.06}_{-0.06}$	$0.64^{+0.09}_{-0.20}$	$0.66^{+0.09}_{-0.10}$
Radiated gravitational-wave energy GV, $M_\odot c^2$	$1.0^{+0.1}_{-0.2}$	$2.0^{+0.6}_{-0.7}$	$1.5^{+0.3}_{-0.4}$
Peak luminosity, erg s^{-1}	$3.3^{+0.8}_{-1.6}\times 10^{56}$	$3.1^{+0.7}_{-1.3}\times 10^{56}$	$3.1^{+0.8}_{-1.8}\times 10^{56}$
Luminosity distance D_L, Mpc	440^{+180}_{-180}	880^{+450}_{-390}	1000^{+500}_{-500}
Redshift z	$0.09^{+0.03}_{-0.04}$	$0.18^{+0.08}_{-0.07}$	$0.20^{+0.09}_{-0.09}$

positively aligned with the orbital angular momentum. This has implications for binary black hole formation channels, as we discuss in the next section.

Notably, a weaker event candidate was also found during the O1 run (October 12, 2015 at 09:54:43 UTC) with a network SNR of 9.7 and a significance of $\lesssim 2\sigma$. More distant than the three confirmed detections at ~ 1000 Mpc ($z \sim 0.2$), parameter estimation indicated that LVT151012[4] was also a binary black hole merger with $\sim 95\%$ probability.

The physical parameters for GW151226, GW170104, and LVT151012 are given in Table 2.

4. Astrophysical implications of the LIGO detections

The gravitational waves detected by LIGO reveal unique insights into the astrophysics of binary black hole systems and indeed black holes themselves. GW150914 provides, for the first time, direct observational proof that binary black hole systems exist and also proves that black hole systems can form, evolve, and merge in Hubble time. The black hole component masses of GW150914 and GW170104 are greater (and in the case of GW150914 significantly greater) than stellar mass black holes found in galactic X-ray binary systems, revealing that stellar mass black holes exist in a broader mass range than previously thought.

The preliminary black hole mass spectrum measured by LIGO has implications for the formation mechanisms and dynamics. Stellar mass binary black hole systems are thought to form through one of two general classes of channels — either dynamical capture in dense stellar environments (such as globular clusters) or via isolated binary formation and evolution through a common envelope phase. A large number of specific model variations exist in each of these two general classes. Heavy stellar mass black holes could form via either channel; however, for isolated binary formation via common-envelope phase the stars' metallicity is likely less than 0.5 times the solar metallicity to prevent a natal kick (an impulsive force) from stellar winds that would drive the binary system apart [13].

[4] The prefix 'LVT' means 'LIGO-Virgo Trigger', a designation that the significance of the event is not sufficient to claim detection by the standard 5σ threshold.

The spins of the initial black holes prior to the merger phase could provide additional clues to binary formation channels. Isolated binary formation mechanisms are likely to have the component spins aligned along the orbital angular momentum plane due to accretion-induced torques, whereas binary systems formed through dynamical capture could possess arbitrarily aligned spins. In general, the spin component of a black hole parallel to the orbital angular momentum leads to changes in the gravitational waveform phase, whilst components in the plane of the orbit produce orbital precession that modulates the emitted waveform. The influence of the individual black hole spins does not predominate the orbital evolution; thus, only weak constraints can be placed on the components' spins from their gravitational waveforms. Using precessing and nonprecessing spin waveform models, we are able to probabilistically infer that if the merging black hole spins have components that are predominantly parallel or anti-parallel to the orbital angular momentum vector. A mass-weighted spin parameter can be defined:

$$\chi_{\rm eff} = m_1 a_1 \cos\vartheta_{\mathbf{LS}_1} + m_2 a_2 \cos\vartheta_{\mathbf{LS}_2}\,, \qquad (3)$$

where $\vartheta_{\mathbf{LS}_{1,2}}$ is the angle between the black hole spin vector $\mathbf{S}_{1,2}$ and the orbital angular momentum vector $\mathbf{L}$. GW151226 is found to have a positive $\chi_{\rm eff} = 0.21^{+0.20}_{-0.10}$, indicating that at least one of the merging black holes had spin $a > 0.2$ with 99% confidence [24]. GW17014 is found to have $\chi_{\rm eff} = -0.12^{+0.21}_{-0.30}$ with a probability of 0.82 that $\chi_{\rm eff}$ is negative, providing the first hints that the spins of at least one of the initial black holes may be anti-parallel to the orbital plane of the binary system.

Our detections allow the first observationally-based estimations of stellar mass black hole merger rates in the universe. Heretofore, merger rates were theoretically predicted from population-synthesis models, with rates ranging from 0.1–300 Gpc^{-3} yr^{-1} spanning more than three orders of magnitude [26]. Using methods described in Ref. [14], much tighter observational constraints can be placed on the rates based on using the four detected events. Two different astrophysically motivated mass-distribution models are assumed — a power law dependency in m_1 and uniform in m_2, and a distribution uniform in the logarithm for both m_1 and m_2. The power law model produces a merger rate estimate of $R = 103^{+110}_{-63}$ Gpc^{-3} yr^{-1}, while the uniform-log model gives $R = 32^{+33}_{-20}$ Gpc^{-3} yr^{-1}, which together produce a combined rate of 12–213 Gpc^{-3} yr^{-1} [24]. These observationally constrained rates are at the upper end of those produced by population-synthesis models and are beginning to rule out specific channels of binary black hole formation mechanisms favoring the more pessimistic merger rates.

The ability to locate the gravitational wave source in the sky with two directors is limited; however, it is possible to determine probabilistic patches of the sky where events occurred. GW150914, GW151226, and GW170104 were localized with error boxes of 230, 850, and 1200 sq. degrees, respectively [20]. Binary black hole mergers are not expected to produce direct counterpart electromagnetic radiation due to the absence of accreting matter at the time of the merger; nonetheless, exotic electromagnetic emission mechanisms have been postulated [27].

Two-detector gravitational wave error boxes are orders of magnitude greater than the typical angular coverage area of telescopes probing the electromagnetic spectrum. While such

large error boxes are difficult to effectively cover on short time scales, follow up campaigns have been conducted for each of the three detections. For GW150914, approximately 25 telescopes spanning from the radio to the X-ray portions of the electromagnetic spectrum targeted specific regions of the gravitational-wave error box, in many cases using 'tiled' observations over day to week time periods to cover larger fractions of the error box. No definitively correlated electromagnetic emissions were observed [28]. Results of electromagnetic follow-up observing campaigns for GW170401 are pending.

5. Conclusion

The detection of gravitational waves, coming almost 100 years after Albert Einstein first predicted them, was made possible by a dedicated and decades-long campaign to build LIGO. The discovery and identification of multiple binary black hole mergers during the first two years of Advanced LIGO observations suggest that gravitational wave astronomy will become the dominant observational tool for studying the dynamics of black holes and the origins of binary black hole formation in the coming years.

LIGO's second observational campaign O2 began in November 2016 and is planned to last through August 2017. The Advanced Virgo detector located in Pisa, Italy is currently being commissioned with the goal of beginning running jointly with LIGO sometime in the summer of 2017.*** By virtue of being the third km-scale gravitational-wave interferometer in operation, Advanced Virgo will significantly improve the localization of gravitational-wave candidates and power, which promises to be a revolution in multi-messenger astronomy. Further along, the 3-km-long underground Japanese KAGRA detector is expected to join the search for gravitational waves late in this decade. LIGO-India, a project underway to locate an Advanced LIGO detector in India, will add further capability to the ground-based gravitational-wave observatory network. Collectively, the five-detector network will be able to localize gravitational-wave events on the sky within a few square degrees, much more precisely than the current precision delivered by the two-detector LIGO-only network.

Beyond black hole mergers, ground-based gravitational wave detectors are actively searching for other compact energetic gravitational-wave producing astrophysical events, including binary neutron star mergers, supernovae, and emissions from isolated rapidly spinning neutron stars. Detections of these types of events will further establish gravitational-wave observatories as a powerful new way of doing astronomy, and may produce paradigm-shifting insights into the nature of the universe.

Acknowledgements

The author gratefully acknowledges support of the US National Science Foundation grants PHY0757058 and PHY0823459. The author is a member of the LIGO Scientific Collaboration, which carried out this work jointly with the Virgo Collaboration. This paper is assigned LIGO document number LIGO-P1700153.

*** Joint observations of two LIGO and VIRGO detectors took place in August 1–August 25, 2017. Two GW events were reported: GW170814 is another binary black hole merging (Abbott B P et al. *Phys. Rev. Lett.* **119** 141101 (2017), and GW170817 is the first detection of binary neutron stars accompanied by detection of electromagnetic radiation from gamma-rays to radio (Abbott B P et al. *Phys. Rev. Lett.* **119** 161101 (2017). (*Editor's note*.)

References

1. Einstein A *Sitzungsber. König. Preuß. Akad. Wiss. Berlin* 688 (1916); Translated into English: *The Collected Papers of Albert Einstein* Vol. 6 *The Berlin Years: Writings, 1914–1917* (Princeton, NJ: Princeton Univ. Press, 1997) p. 201
2. Kennefick D *Traveling at the Speed of Thought: Einstein and the Quest for Gravitational Waves* (Princeton, NJ: Princeton Univ. Press, 2007)
3. Weber J *Phys. Rev.* **117** 306 (1960)
4. Gertsenshtein M E, Pustovoit V I *Sov. Phys. JETP* **16** 433 (1963); *Zh. Eksp. Teor. Fiz.* **43** 605 (1962)
5. Weiss R "Electromagnetically coupled broadband gravitational antenna", Quarterly Progress Report No. 105 (Cambridge, MA: Massachusetts Institute of Technology, Research Laboratory of Electronics, 1972); https://dcc.ligo.org/LIGO-P720002/public/main
6. Drever R W P, in *Gravitational Radiation* (Eds N Deruelle, T Piran) (Amsterdam: North-Holland, 1983) p. 321
7. Vogt R E et al. "A Laser Interferometer Gravitational-Wave Observatory (LIGO)", Technical Report (Cambridge, MA: Massachusetts Institute of Technology, 1989); https://dcc.ligo.org/LIGO-M890001/public/main
8. Abbott B P et al. (LIGO Scientific Collab. and Virgo Collab.) *Phys. Rev. Lett.* **116** 061102 (2016)
9. Aasi J et al. (LIGO Scientific Collab. and Virgo Collab.) *Class. Quantum Grav.* **32** 074001 (2015)
10. Abbott B P et al. (LIGO Scientific Collab. and Virgo Collab.) *Phys. Rev. Lett.* **116** 131103 (2016)
11. Klimenko S et al. *Phys. Rev. D* **93** 042004 (2016)
12. Abbott B P et al. (LIGO Scientific Collab. and Virgo Collab.) *Class. Quantum Grav.* **33** 134001 (2016)
13. Abbott B P et al. (LIGO Scientific Collab. and Virgo Collab.) *Astrophys. J. Lett.* **818** L22 (2016)
14. Abbott B P et al. (LIGO Scientific Collab. and Virgo Collab.) *Astrophys. J. Lett.* **833** L1 (2016)
15. Abbott B P et al. (LIGO Scientific Collab. and Virgo Collab.) *Phys. Rev. Lett.* **116** 241102 (2016)
16. Abbott B P et al. (LIGO Scientific Collab. and Virgo Collab) *Phys. Rev. Lett.* **116** 221101 (2016)
17. Dal Canton T et al. *Phys. Rev. D* **90** 082004 (2014)
18. Privitera S et al. *Phys. Rev. D* **89** 024003 (2014)
19. Allen B *Phys. Rev. D* **71** 062001 (2005)
20. Abbott B P et al. (LIGO Scientific Collab. and Virgo Collab) *Phys. Rev. X* **6** 041015 (2016)
21. Aasi J et al. (LIGO Scientific Collab. and Virgo Collab) *Phys. Rev. D* **88** 062001 (2013)
22. Wex N, arXiv:1402.5594
23. Del Pozzo W, Veitch J, Vecchio A *Phys. Rev. D* **83** 082002 (2011)
24. Abbott B P et al. (LIGO Scientific Collab. and Virgo Collab.) *Phys. Rev. Lett.* **116** 241103 (2016)
25. Abbott B P et al. (LIGO Scientific Collab. and Virgo Collab.) *Phys. Rev. Lett.* **118** 221101 (2017)
26. Abadie J et al. (LIGO Scientific Collab. and Virgo Collab.) *Class. Quantum Grav.* **27** 173001 (2010)
27. Loeb A *Astrophys. J. Lett.* **819** L21 (2016)
28. Abbott B P et al. (LIGO Scientific Collab. and Virgo Collab., Australian Square Kilometer Array Pathfinder (ASKAP) Collab., BOOTES Collab., Dark Energy Survey and Dark Energy Camera GW-EM Collab., Fermi GBM Collab., GRAvitational Wave Inaf TeAm (GRAWITA), INTEGRAL Collab., Intermediate Palomar Transient Factory (iPTF) Collab., InterPlanetary Network, J-GEM Collab., La Silla-QUEST Survey, Liverpool Telescope Collab., Low Frequency Array (LOFAR) Collab., MASTER Collab., MAXI Collab., Murchison Wide-field Array (MWA) Collab., Pan-STARRS Collab., PESSTO Collab., Pi of the Sky Collab., Sky-Mapper Collab., Swift Collab., TAROT, Zadko, Algerian National Observatory, and C2PU Collab., TOROS Collab., and VISTA Collab.) *Astrophys. J. Lett.* **826** L13 (2016)